THE JOURNAL OF PHYSICAL CHEMISTRY C LETTERS

2009, *113,* 15788–15791
Published on Web 08/17/2009

Template-Free Electrochemical Growth of Single-Crystalline Zinc Nanowires at an Anomalously Low Temperature

Debabrata Pradhan, Shrey Sindhwani, and K. T. Leung*

WATLab and Department of Chemistry, University of Waterloo, Waterloo, Ontario N2L 3G1, Canada

Received: July 01, 2009; Revised Manuscript Received: August 11, 2009

Zinc nanowires of serpentine geometry have been grown on conducting plastic and glass substrates in an aqueous electrolyte at an anomalously low temperature of 0 °C by a one-step, template-free electrodeposition technique. These nanowires are of several micrometers long and with a diameter of 20−200 nm. These nanowires are also single-crystalline and found to be coated with a 5 nm thick ZnO shell with an epitaxial relationship to the Zn core.

Metallic nanowires are one of the important classes of nanomaterials with a wide range of technological applications.[1,2] Of the several common growth methods for metallic nanowires, thermal evaporation and electrochemical deposition have been extensively used because of their simplicity and low-cost advantage. Unlike thermal evaporation that often requires a relatively high temperature (>500 °C) to prepare nanowires, electrodeposition is usually carried out at a considerably lower temperature, from room temperature to 90 °C, making it a more attractive technique for substrates with lower heat tolerance (e.g., polymers and plastics). In most cases, one or multiple metals are electrodeposited into a template, such as anodic aluminum oxide, which is subsequently dissolved in a solution to harvest the nanowires.[3,4] More recently, Penner and co-workers have introduced new techniques to synthesize polycrystalline nanowires of several noble metals horizontally decorated on substrates by using either electrochemical step edge decoration or lithographically patterned nanowire electrodeposition.[5] In the present work, we demonstrate, for the first time, the growth of single-crystalline metallic zinc (Zn) nanowires at an even lower temperature of 0 °C by a direct electrodeposition technique without using any template, thus making the synthesis not only a facile, one-step process but also appropriate for integration with biological materials. These nanowires could exhibit intriguing properties, including metal−insulator transitions, one-dimensional superconductivity, and better performance in alkaline battery applications. For instance, Tian et al. have recently reported the unique superconducting behavior of Zn nanowires (obtained by an electrodeposition method using an anodic aluminum oxide template), while Heremans et al. characterized the magnetoresistance and thermopower of Zn nanowire composites (synthesized by thermal evaporation).[6,7]

To date, Zn nanowires have been primarily synthesized by using thermal evaporation,[8] which involves evaporation of a Zn, ZnO, or ZnS precursor at 580−1400 °C and condensation to Zn nanowires in the colder region of the chamber (200−300 °C). Less popular methods such as spray pyrolysis,[9] carbothermal reduction,[10] cold-wall deposition,[11] and ECR plasma deposition[12] have also been used to produce Zn nanowires on a substrate at 150−300 °C. There are only a few reports of Zn nanowire formation by wet-chemistry techniques, such as hydrothermal synthesis at 150 °C,[13] HF etching,[14] and template-assisted electrodeposition at room temperature.[15,16] The present work provides the first results of synthesizing single-crystalline Zn nanowires not only in a single step and without the use of template but also below room temperature. The formation of Zn nanowires at 0 °C demonstrated in the present work promises new opportunities in developing biologically active ("live") nanocomposites,[17] and applications requiring low-heat tolerant substrates such as low-cost plastics. Bacteria, viruses, and biomolecules have been shown to be capable of ordering inorganic nanocrystals into novel nanoarchitectures.[18] As most viruses and biomolecules are known to become less stable above room temperature,[19] there is great interest in developing this type of low-temperature growth procedure to allow in situ incorporation of "living" species into nanomaterials without the risk of denaturing.

In electrochemical synthesis, the types and concentrations of the electrolytes, the deposition potential, and the deposition temperature can all be used to control the structure, shape, size, and crystal quality of the Zn nanostructured materials.[16,20] In most cases, a template is used to electrochemically synthesize a particular type of Zn nanostructures. For example, zinc inverted opals have been fabricated at room temperature using a polystyrene template,[21] and in a very recent study, Gao et al. deposited zinc nanoparticles on indium tin oxide (ITO) coated glass at 70 °C via a metal−ligand-coordinated vesicle phase.[22] In the present work, direct electrodeposition was carried out in a conventional three-electrode glass cell placed in a temperature bath held at 0 °C without use of any type of template. A Ag/AgCl electrode was used as the reference, while a spiral platinum wire served as the counter electrode. The working electrode was either a In_2O_3/Au/Ag coated polyethylene terephthalate (PET) or an ITO coated glass substrate, with a resistance of $\leq 10\ \Omega$. A CH Instruments 660A potentio/galvanostat electrochemical workstation was used to deposit the Zn nanowires with the deposition potential held at either −1.4 or −1.5 V (relative to the Ag/AgCl reference electrode), in an aqueous

* To whom correspondence should be addressed. E-mail: tong@uwaterloo.ca.

10.1021/jp906198h CCC: $40.75

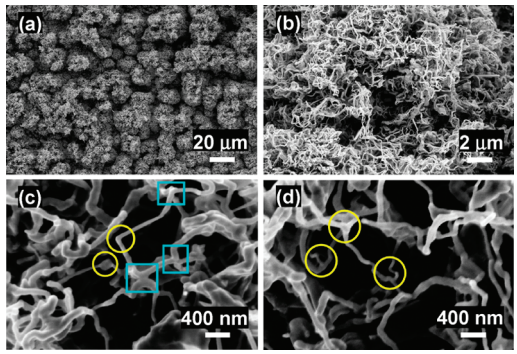

Figure 1. (a, b) SEM images of nanowires electrodeposited in 0.1 M $Zn(NO_3)_2 \cdot 6H_2O$ on a conducting PET substrate at 0 °C. Magnified views of (c) L-, V-, and multijunctions, and (d) T- and Y-junctions of nanowires.

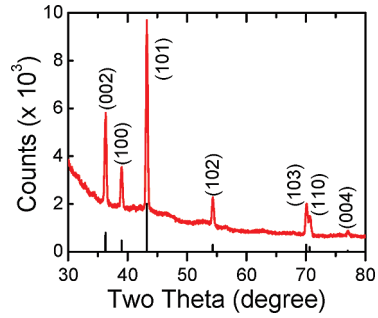

Figure 2. GIXRD spectrum of nanowires electrodeposited in 0.1 M $Zn(NO_3)_2 \cdot 6H_2O$ on a conducting PET substrate at 0 °C, along with a bar chart of the reference spectrum of Zn (JCPDS 01-087-0713). The crystallographic planes of the Zn nanowires are labeled.

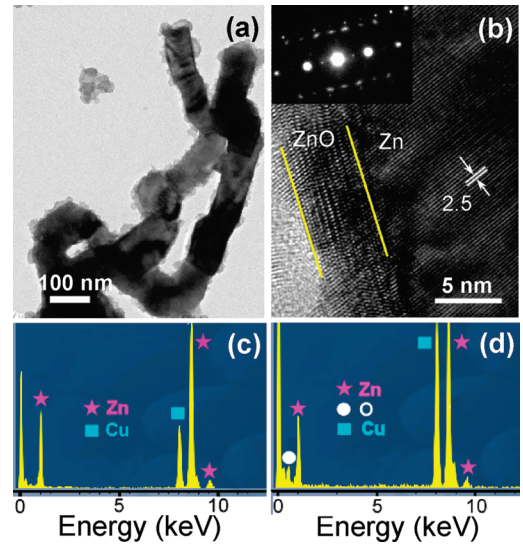

Figure 3. (a) Low-magnification and (b) high-resolution TEM images of a nanowire, depicting the Zn central core region and the ZnO exterior. The corresponding electron diffraction pattern (inset of b) clearly shows two sets of parallel single-crystalline diffraction spots indexed to Zn and ZnO. EDX spectra collected from the (c) central and (d) outer regions of a nanowire. The presence of the Cu feature is due to the TEM grid on which the samples were mounted.

electrolyte solution of 0.1 M $Zn(NO_3)_2 \cdot 6H_2O$ (Aldrich). The overall surface morphologies of electrodeposits were examined by a LEO FESEM 1530 field-emission scanning electron microscope (SEM). The glancing-incidence X-ray diffraction (GIXRD) data was collected by using a PANalytical X'Pert Pro MRD diffractometer with Cu Kα radiation (1.54 Å) and an incidence angle of 0.3°. Transmission electron microscopy (TEM) measurements were performed using a JEOL 2010 transmission electron microscope with an operating accelerating voltage of 200 kV. The surface composition of the Zn nanowires was further analyzed by X-ray photoelectron spectroscopy (XPS) using a Thermo-VG Scientific ESCALab 250 Microprobe with a monochromatic Al Kα source (1486.6 eV), capable of an energy resolution of 0.4−0.5 eV full width at half-maximum.

The SEM images shown in Figure 1 illustrate the morphologies of Zn nanowires obtained by direct electrodeposition on a conducting In_2O_3-coated PET substrate at −1.4 V (with respect to a Ag/AgCl reference) in a 0.1 M $Zn(NO_3)_2 \cdot 6H_2O$ electrolyte. Similar results were obtained with a deposition potential of −1.5 V. Evidently, entangled nanowires with sections of nonuniform diameters over the length (Figure 1b) are found to organize into fibrous globular agglomerations, shown in Figure 1a. These nanowires are several micrometers long, with the diameter in the range 20−200 nm (Figure 1c,d). These nanowires not only are curvy with a serpentine geometry but also show abrupt bending at various angles forming L-, V-, and multibranch junctions (Figure 1c), as well as T- and Y-junctions (Figure 1d). While the origin of these junctions is unclear, we speculate that they could be related to the formation of defects and/or a secondary phase such as ZnO during growth. Zn nanowires with a similar entangled geometry have also been previously obtained on silicon, quartz, and alumina but at a considerably higher temperature range of 580−1225 °C by thermal evaporation.[8] The present work therefore shows, for the first time, that growth of such Zn nanowires is possible even at 0 °C. If the deposition was carried out at room temperature without changing other deposition conditions, we obtained a porous film (not shown). Furthermore, the use of a less negative deposition potential (−1.0 to −1.3 V) also did not produce the observed nanowires. The use of higher electrolyte concentrations produced nonuniform films consisting of both nanowires and submicrometer-sized grains (0.5 μm). These results therefore suggest that the deposition temperature, potential, and electrolyte concentration all play a crucial and interdependent role in the formation of nanowires.

Figure 2 shows the corresponding GIXRD pattern of the electrodeposits on PET. The diffraction peaks can be indexed to the hexagonal crystal structure of Zn (space group $P6_3/mmc$) with lattice constants $a = b = 2.6637$ Å and $c = 4.9430$ Å, which are in good accord with the reference Zn lattice constants ($a = b = 2.6650$ Å and $c = 4.9570$ Å, JCPDS file 01-087-0713). It should be noted that, despite the use of the glancing-incidence mode for our XRD measurement, no diffraction peak attributable to ZnO is observed, suggesting that the nanowires consist primarily of Zn metal, and the concentration of any residual component such as ZnO, if present, is below the (bulk) detection limit of X-ray diffraction. Similar diffraction features can also be obtained from Zn nanowires in a conventional powder XRD measurement but with a considerably higher intensity due to a larger sampling volume. No new feature (e.g., ZnO) has also been observed 6 months after the sample was first prepared, indicating that the nanowires consist primarily of a metallic Zn core with a very thin passivating (ZnO) shell (discussed below).

Figure 3a shows a typical TEM image of nanowires obtained in the present work. The abrupt bending and multiple sections of these nanowire structures are clearly evident. The corresponding high-resolution TEM image (Figure 3b) reveals a 4−5 nm thick coating of ZnO on the central Zn nanowire core. The Zn nanowire exhibits distinct fringes corresponding to an

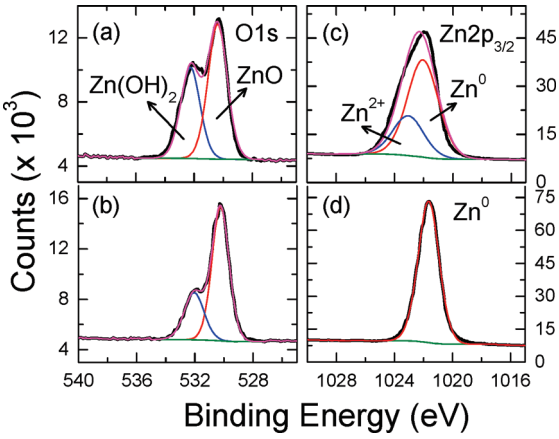

Figure 4. XPS spectra of (a, b) O 1s and (c, d) Zn $2p_{3/2}$ regions of nanowires, as electrodeposited in 0.1 M $Zn(NO_3)_2 \cdot 6H_2O$ on a conducting PET substrate at 0 °C, collected after argon ion sputtering for (a, c) 60 s and (b, d) 600 s.

interplanar spacing of 2.5 Å, in good accord with the separation between the (0001) crystal planes of hexagonal Zn. This indicates that the Zn nanowires grow along the [0001] direction corresponding to the *c*-axis of hexagonal Zn. The outer region of the nanowire exhibits a lattice pattern matching to hexagonal ZnO. Given the similar hexagonal crystal structures of Zn and ZnO and the small lattice mismatch of ~5%, it is not surprising to observe that the growth of the ZnO shell follows an epitaxial orientation relationship with the Zn core, as shown by the presence of two sets of parallel diffraction spots (inset of Figure 3b) indexed to Zn(0001) and ZnO(0001). Similar core−shell nanostructures but with different crystal orientations have been reported for the case of Zn−ZnO core−shell nanotubes and nanobelts synthesized by using the thermal evaporation technique (at a considerably higher temperature of 1350 °C).[23] This suggests that crystal orientation is directly dependent on the type of Zn nanostructure, which in turn depends on their synthesis methods and parameters. The absence and presence of the O K_α feature in the energy dispersive X-ray (EDX) spectra collected from, respectively, the central region (Figure 3c) and exterior of the nanowires (Figure 3d) further confirm the chemical compositions of Zn and ZnO in the respective parts of the nanowires.

The surface chemical composition of as-synthesized nanowires is further analyzed by XPS. Figure 4 shows XPS spectra of the O 1s and Zn $2p_{3/2}$ regions for the nanowires after 60 and 600 s argon ion sputtering. The O 1s envelope (Figure 4a,b) can be fitted to a $Zn(OH)_2$ component at 532.0 eV and a ZnO component at 530.3 eV. $Zn(OH)_2$ is known to form as an intermediate in the hydroxylation step for the formation of ZnO,[20] and it usually presents as a thin amorphous overlayer on top of the ZnO. The Zn $2p_{3/2}$ feature after 60 s of sputtering can be fitted to two components at 1023.0 eV for Zn^{2+} and 1022.0 eV for Zn^0 (Figure 4c). After 600 s of sputtering, only the metallic Zn peak (Zn^0) is obtained at 1021.8 eV (Figure 4d),[24] confirming the removal of the ZnO shell after sputtering.

In an aqueous solution of $Zn(NO_3)_2 \cdot 6H_2O$, the Zn^{2+} ions can be easily reduced to Zn metal on the substrate surface of the working (PET) electrode, with the standard reduction potential of Zn^{2+} to Zn being −0.76 V vs standard hydrogen electrode at standard temperature and pressure conditions. Zinc metal is known to be deposited electrochemically at a higher negative applied potential (i.e., more negative than −1.0 V but less negative than the hydrogen evolution potential of −1.8 V, both with respect to Ag/AgCl) at room temperature.[21] However, at a higher deposition temperature, metallic Zn is easily corroded and converted to the more passive ZnO phase via the following reaction:

$$Zn(s) + H_2O(l) \rightleftarrows ZnO(s) + H_2(g)$$

Similarly, at a lower applied potential (e.g., −0.7 V), the growth rate is slower than the corrosion rate and therefore the deposited Zn is converted to ZnO.[15]

In the present work, the application of a higher negative deposition potential (−1.4 to −1.5 V vs Ag/AgCl reference) not only allows the Zn^{2+} ions to be reduced to Zn metal but also accelerates the growth along the *c*-axis of Zn to produce nanowires, despite the expected slower reaction kinetics at 0 °C. The formation of ZnO is not favored under these conditions because of the low conductivity of the electrolyte (due to the lack of any supporting electrolyte such as KCl), slow kinetics, and low corrosion rate at low temperature.[25] A high deposition temperature (75 °C) and a high negative potential (e.g., −1.5 V, the same as that used in the present work) can produce a polycrystalline Zn−ZnO composite structure, in which the nanowire is composed of alternating Zn and ZnO grains, as obtained by Wang et al. using an anodized aluminum oxide template.[15] Once the application of the deposition potential is terminated, the surface of as-formed Zn nanowires, being still inside the aqueous solution, is converted to ZnO either via the $Zn(OH)_2$ intermediate or directly by air oxidation when the nanowire sample is taken out to the ambient room temperature. To date, formation of nanowires below room temperature or at less negative deposition potentials has not been reported. The formation of nanowires at 0 °C in the present work can therefore be attributed to the combined effect of deposition temperature, potential, and electrolytes, all of which provide a delicate balance in controlling the nucleation and kinetics of electrodeposition.

In summary, we demonstrate that Zn nanowires can be grown, for the first time, at 0 °C on a conducting PET (or ITO-glass) substrate by a template-free, direct electrodeposition method. These nanowires consist of sections of nonuniform diameter (in the range 20−200 nm) over the length, and exhibit numerous bends and turns at different angles and junctions with double and triple (and multiple) branches. XRD confirms the hexagonal crystal structures of these Zn nanowires. TEM study clearly shows not only an ~5 nm thick ZnO layer on the surface of Zn nanowires but also an epitaxial relationship between the ZnO shell and Zn core of the nanowires (due to their similar crystal structures). XPS measurement further validates the composition of the Zn nanowires with a ZnO shell. The present work opens up the possibility of direct integration of biologically active materials without denaturing into these nanowires at 0 °C, which promise novel properties for new applications.

Acknowledgment. This work was supported by the Natural Sciences and Engineering Research Council of Canada.

References and Notes

(1) Li, M.; Bhiladvala, R. B.; Morrow, T. J.; Sioss, J. A.; Lew, K.-K.; Redwing, J. M.; Keating, C. D.; Mayer, T. S. *Nat. Nanotechnol.* **2008**, *3*, 88.

(2) Singh, A.; Sai, T. P.; Ghosh, A. *Appl. Phys. Lett.* **2008**, *93*, 102107.

(3) Drury, A.; Chaure, S.; Kroell, M.; Nicolosi, V.; Chaure, N.; Blau, W. J. *Chem. Mater.* **2007**, *19*, 4252.

(4) Tian, M.; Wang, J.; Kumar, N.; Han, T.; Kobayashi, Y.; Liu, Y.; Mallouk, T. E.; Chan, M. H. W. *Nano Lett.* **2006**, *6*, 2773.

(5) Xiang, C.; Kung, S. -C.; Taggart, D. K.; Yang, F.; Thompson, M. A.; Güell, A. G.; Yang, Y.; Penner, R. M. *ACS Nano* **2008**, *2*, 1939.

(6) Tian, M.; Kumar, N.; Wang, J.; Xu, S.; Chan, M. H. W. *Phys. Rev. B* **2006**, *74*, 014515.

(7) Heremans, J. P.; Thrush, C. M.; Morelli, D. T.; Wu, M.-C. *Phys. Rev. Lett.* **2003**, *91*, 076804.

(8) Kar, S.; Ghoshal, T.; Chaudhuri, S. *Chem. Phys. Lett.* **2006**, *419*, 174, and references therein.

(9) Vivekchand, S. R. C.; Gundiah, G.; Govindaraj, A.; Rao, C. N. R. *Adv. Mater.* **2004**, *16*, 1842.

(10) Yan, Y.; Liu, P.; Romero, M. J.; Al-Jassim, M. M. *J. Appl. Phys.* **2003**, *93*, 4807.

(11) Kast, M.; Schroeder, P.; Hyun, Y. J.; Pongratz, P.; Brucekl, H. *Nano Lett.* **2007**, *7*, 2540.

(12) Purohit, V. S.; Dey, S.; Bhattacharya, S. K.; Kshirsagar, A.; Dharmadhikari, C. V.; Bhoraskar, S. V. *Nucl. Instrum. Methods Phys. Res., Sect. B* **2008**, *266*, 4980.

(13) Hu, J.; Chen, Z.; Xie, J.; Yu, Y. *J. Phys. D: Appl. Phys.* **2008**, *41*, 032004.

(14) Chang, S. -S.; Yoon, S. O.; Park, H. J.; Sakai, A. *Mater. Lett.* **2002**, *53*, 432.

(15) Wang, J. -G.; Tian, M. -L.; Kumar, N.; Mallouk, T. E. *Nano Lett.* **2005**, *5*, 1247.

(16) Wang, Y.; Zhao, H.; Hu, Y.; Ye, C.; Zhang, L. *J. Cryst. Growth* **2007**, *305*, 8.

(17) Riegler, J.; Ditengou, F.; Palme, K.; Nann, T. *J. Nanobiotechnol.* **2008**, *6*, 7.

(18) Tseng, R. J.; Tsai, C.; Ma, L.; Ouyang, J.; Ozkan, C. S.; Yang, Y. *Nat. Nanotechnol.* **2006**, *1*, 72.

(19) Flint, K. P. *J. Appl. Bacteriol.* **1987**, *63*, 261.

(20) Pradhan, D.; Leung, K. T. *Langmuir* **2008**, *24*, 9707.

(21) Juarez, B. H.; Lopez, C.; Alonso, C. *J. Phys. Chem. B* **2004**, *108*, 16708.

(22) Gao, Y.; Hao, J. *J. Phys. Chem. B* **2009**, *113*, 9461.

(23) Kong, X. Y.; Ding, Y.; Wang, Z. L. *J. Phys. Chem. B* **2004**, *108*, 570.

(24) Moulder, J. F.; Stickle, W. F.; Sobol, P. E.; Bomben, K. D. In *Handbook of X-ray Photoelectron Spectroscopy*; Chastain, J., Ed.; Perkin-Elmer Corporation: Eden Prairie, MN, 1992.

(25) Pradhan, D.; Leung, K. T. *J. Phys. Chem. C* **2008**, *112*, 1357.

JP906198H